

## Continuum approach of physical line structures with applications to high polymers and to flux line lattices of superconductors(\*)

K. H. ANTHONY (STUTTGART)

A THREE-DIMENSIONAL, nonlinear, local field theory describing ordered physical line structures was established. This theory allows for arbitrary configurations of the system. In particular, eigenstress-states associated with structure defects such as dislocations and disclinations may be investigated. The lecture treats the following topics: 1) fundamental ideas of the theory, 2) defects in the ordered line bundle, 3) realization of the theory by the bundle model of high polymers, 4) realization of the theory by the magnetic flux line lattice of superconductors. In order to take into account interaction effects between the atomic lattice and the flux line lattice the theory has to be generalized. This generalization is associated with the model: ordered line bundle embedded into a point lattice.

Sformułowano trójwymiarową, nieliniową lokalną teorię opisującą uporządkowane struktury utworzone z linii fizycznych. Teoria ta dopuszcza dowolne konfiguracje układu. W szczególności w ramach tej teorii mogą być rozważane stany naprężeń własnych stowarzyszone z takimi defektami strukturalnymi, jak dyslokacje i dysklinacje. W pracy rozważono następujące zagadnienia: 1) główne idee pracy, 2) defekty w uporządkowanej wiązce linii, 3) realizacja teorii przez model wiązki polimerów, 4) realizacja teorii przez sieć utworzoną przez linie strumienia pola magnetycznego nadprzewodników. Aby było możliwe uwzględnienie oddziaływania między siecią atomową i siecią linii prądu należało teorię uogólnić. Uogólnienie takie oparte jest na modelu uporządkowanej wiązki linii wmrózonej w sieć punktową.

Сформулирована трехмерная, нелинейная локальная теория описывающая упорядоченные структуры образованные из физических линий. Эта теория допускает произвольные конфигурации системы. В частности в рамках этой теории могут рассматриваться состояния собственных напряжений ассоциированные с такими структурными дефектами, как дислокации и дискликации. В работе обсуждены следующие вопросы: 1) главные положения работы, 2) дефекты в упорядоченном пучке линий, 3) реализация теории моделью пучка полимеров, 4) реализация теории сеткой образованной линиями потока магнитного поля сверхпроводников. Чтобы можно было учесть взаимодействия между атомной решеткой и сеткой линий тока следовало бы обобщить теорию. Такое обобщение опирается на модель упорядоченного пучка линий в замороженной в точечную решетку.

### 1. Introductory remarks

THE CLASSICAL field theory as based on the methods of non-Euclidean geometries is capable of describing arbitrary configurations of ordered material structures. The physical elements of the most fundamental ordered structures are points, lines and sheets, where the lines and sheets exhibit no inherent physical structure at all. According to these elements we get point lattices, ordered line bundles and ordered layer structures (Fig. 1).

Apart from the atomic crystals the magnetic flux line lattice of superconductors get another prominent realization of the point lattice, which is of current physical interest.

(\*) Manuscript of a lecture given at the Conference on "Continuum Model of Discrete Systems", Jodłowy Dwór, Poland, June 1975.

Whereas the atomic lattice is three-dimensional, the flux line lattice is a two-dimensional lattice occurring in cross-sections of a straight flux line bundle (Fig. 2). The classical field theory has proved to be a powerful tool for describing deformed configurations of point lattices. The deformations may be due to external body and surface forces as well as to structure defects of the lattice [2-12] or to deformation sources summarized by the notion

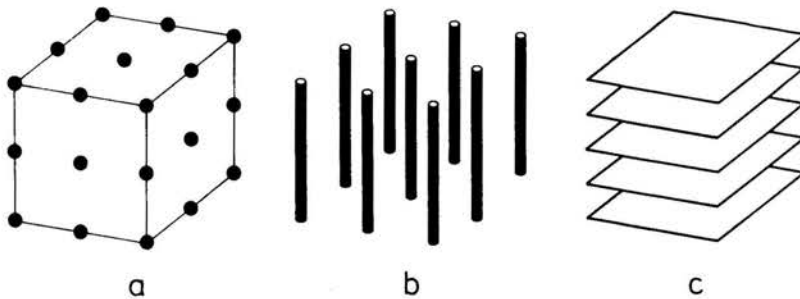


FIG. 1. Ordered material structures: a) point lattice, b) ordered line bundle, c) ordered layer structure,

“quasi-plastic deformations” [13, 14]<sup>(1)</sup>. It is a well-known fact that a variety of macroscopic as well as microscopic properties of a crystal lattice can be understood by means of structure defects [15] and by their mutual elastic interactions on the microscale. Let us recall here dislocations [16] which are closely correlated with plasticity and with work hardening [17].

It is quite natural to look for the same problems in the case of ordered line bundles and of ordered layer structures. Three-dimensional line bundles are physically realized for instance in the magnetic flux line lattice of superconductors [1, 18]<sup>(2)</sup> and in the bundle



FIG. 2. Two-dimensional magnetic flux line lattice of superconductors, undeformed configuration (Micrograph due to TRÄUBLE and ESSMANN [1]).

model of high polymers [19]. Layer structures are found for instance in cholesteric and smectic liquid crystals [20]. All these structures can be deformed; in all structures we may introduce structure defects, a lot of which are really observed. As in the case of point lattices we ask if it is possible to understand the macroscopic as well as microscopic behaviour

<sup>(1)</sup> For instance: thermal strains due to a temperature gradient.

<sup>(2)</sup> The flux line bundle may be described completely by means of a two-dimensional point lattice only if the flux lines are straight and parallel [36].

of these systems by means of certain structure defects and by their mutual interactions [21, 23]. Restricting my lecture to the magnetic flux line lattice of superconductors and to the bundle model of high polymers I shall try to explain these problems and their correlation to the classical field theory.

To start with a guide for the case of the ordered line bundle let us have a glance at the methodical relationship between a discrete point lattice and its associated field theory: On the one hand, structure defects are singularities in the physical system disturbing the regular topology of the discrete lattice and giving rise to elastic eigenstrains of the lattice. To give an example, Fig. 3 shows an edge-dislocation, the topology of which is characterized by open lattice parallelograms. The closure failure is called the Burgers vector of the dislocation. On the other hand a main problem of the mathematical field theory is to cal-

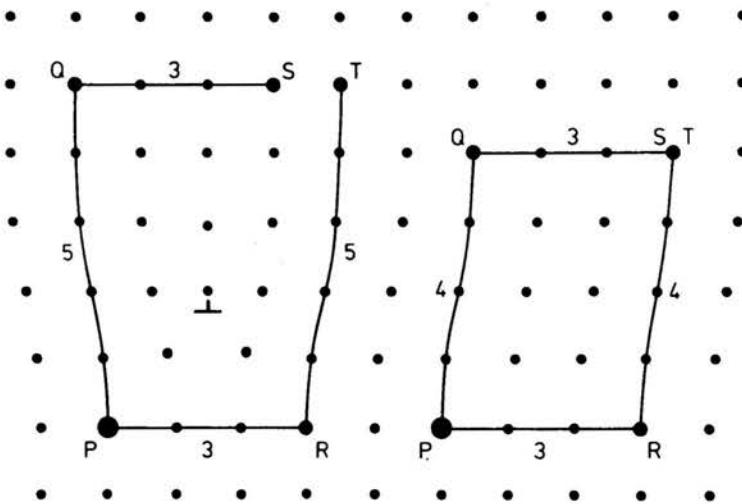


FIG. 3. Edge dislocation in a cubic point lattice. Lattice parallelograms are built up by means of two pairs of equivalent lattice lines. The two lines of each pair exhibit the same length as measured by means of lattice spacings. Only those parallelograms are closed, which do not enclose the dislocation.

culate sufficiently continuous fields which are associated with given singularities. Such singularities may be sources or vortices or more complicated ones. It is evident that this problem is quite analogous to the problem of physical singularities. Therefore, we try to fit the mathematical singularities and their corresponding fields as well as possible to the physical singularities and their associated lattice strains. Nevertheless, we are really dealing with a discrete physical system and we rather associate a continuum model with this system. The accuracy of the results calculated by means of the model depends on the accuracy of the original fitting procedure. If this procedure takes place on the microscale, i.e. if it takes sufficiently into account the microstructure of the system, we may expect good results even on the microscale. The fitting procedure has to take care of the system's topology as well as of its energy content. The outcome of the fitting procedure is a set of compatibility equations, referring to the topology of the system, and a set of equilibrium and constitutive equations, referring to the material response of the system.

Let us look again at the dislocation of Fig. 3. It is a well-known fact that a point lattice is well fitted by means of a continuum model which is endowed with a parallelism [11]. This "lattice parallelism" is a continuous operation within the continuum model. It is associated with the natural displacement of a lattice vector within the discrete lattice (Fig. 4a), i.e. lattice vectors are parallelly displaced with respect to the lattice parallelism. If the torsion of this parallelism does not vanish, we get a non-Euclidean parallelism which is characterized by open parallelograms (Fig. 4b) [24]. If we choose the torsion tensor

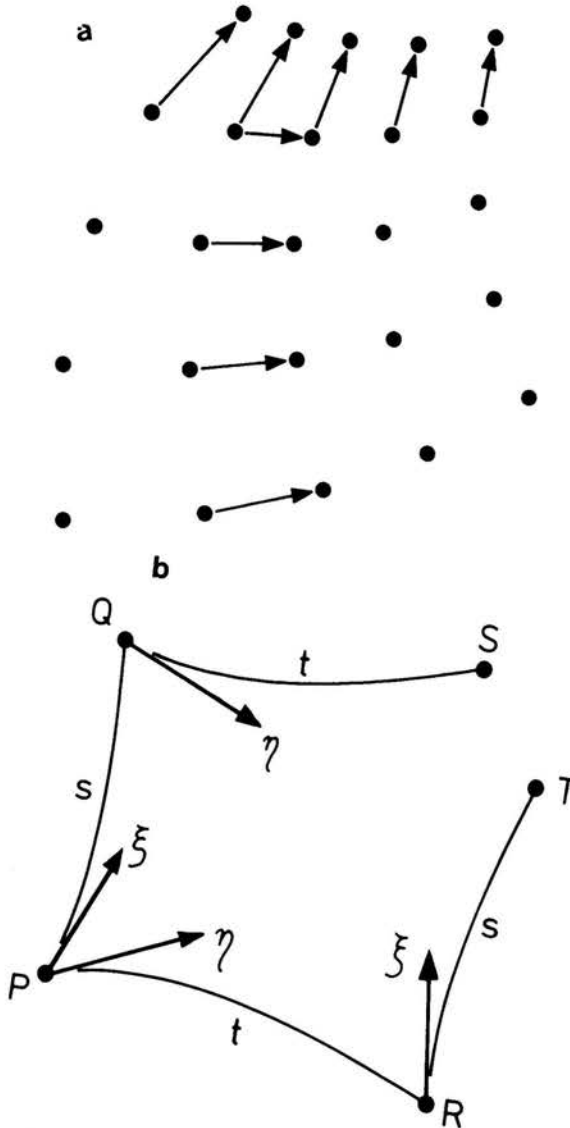


FIG. 4. a) Lattice parallelism  $\Gamma$ . b) A parallelism  $\Gamma$  with torsion produces open parallelograms. The parallelogram consists of two pairs of autoparallel lines. Opposite sides, being parallel with respect to the  $\Gamma$ -parallelism, exhibit the same length (as measured by means of an appropriate metric [11]).

of the lattice parallelism to be singular along the dislocation line and to vanish elsewhere (i.e. torsion tensor = two-dimensional Dirac's  $\delta$ -function), we are able to fit the open lattice parallelograms of Fig. 3. Basing on this model the eigenstrains of the dislocation have been calculated with sufficient accuracy even on the microscale. Such calculations are the foundations on which calculations of the interaction of different dislocations are based.

Recently I was successful in the analogous program concerning the ordered line bundle [25]. It is possible to associate a continuum model with this discrete system, too, and to fit the model to bundle defects. In order to get a well-fitted continuum model we have first to study the physical system in some detail.

## 2. The magnetic flux line lattice in type II superconductors. Phenomena relevant to the field theory

When a superconducting material<sup>(3)</sup> is cooled down below its critical temperature<sup>(4)</sup>, it is found in its superconducting state where its electrical conductivity gets infinite. Putting a long cylindrical specimen of such a superconducting material into a homogeneous magnetic field  $H$ , we get a magnetization curve which is quite different from those of materials with normal conductivity (Fig. 5a)<sup>(5)</sup> [18]. It is characterized by two critical fields. Below the first critical field  $H_{c1}$  there is absolutely no magnetic flux in the specimen (Fig. 5b). This state in which the specimen is a perfect diamagnet is called the Meissner-state of the superconductor.

Raising the excitation field  $H$  we find at the first critical field a more or less spontaneous penetration of the magnetic flux according to a flux density  $B_0$ . But this flux is not homogeneously distributed. Instead, we find a periodic flux distribution and the flux is mainly located at the flux lines which arrange themselves in an ordered line bundle (Figs. 5c, d). The regular undeformed flux line lattice occurring in cross-sections of the bundle can be visualized on the top surface by means of the electron microscope after having decorated the surface with iron particles (Fig. 2). In general, we find a hexagonal triangle lattice with a lattice constant of the order 5000 Å.

If the exciting magnetic field is further raised, the flux density increases. This happens by means of additional flux lines which are produced in a thin surface layer of the specimen and which migrate into the interior of the specimen. This process is accompanied by an increasing homogeneous compression of the flux line lattice. Due to the elementary flux quantum  $\phi_0 = \frac{hc}{2e}$  <sup>(6)</sup> located at each flux line, the increase of flux density is in a one-to-one correspondence to the decrease of the lattice constant.

At the upper critical field  $H_{c2}$  the very strongly compressed flux line lattice finally

<sup>(3)</sup> For instance Nb, V.

<sup>(4)</sup> Typical values of this temperature are of the order of 10 K and smaller.

<sup>(5)</sup> Type I superconductors exhibit a different behaviour. They can be transformed into type II superconductors by means of admixtures.

<sup>(6)</sup>  $h$  — Planck's constant,  $e$  — electron charge,  $c$  — speed of light.

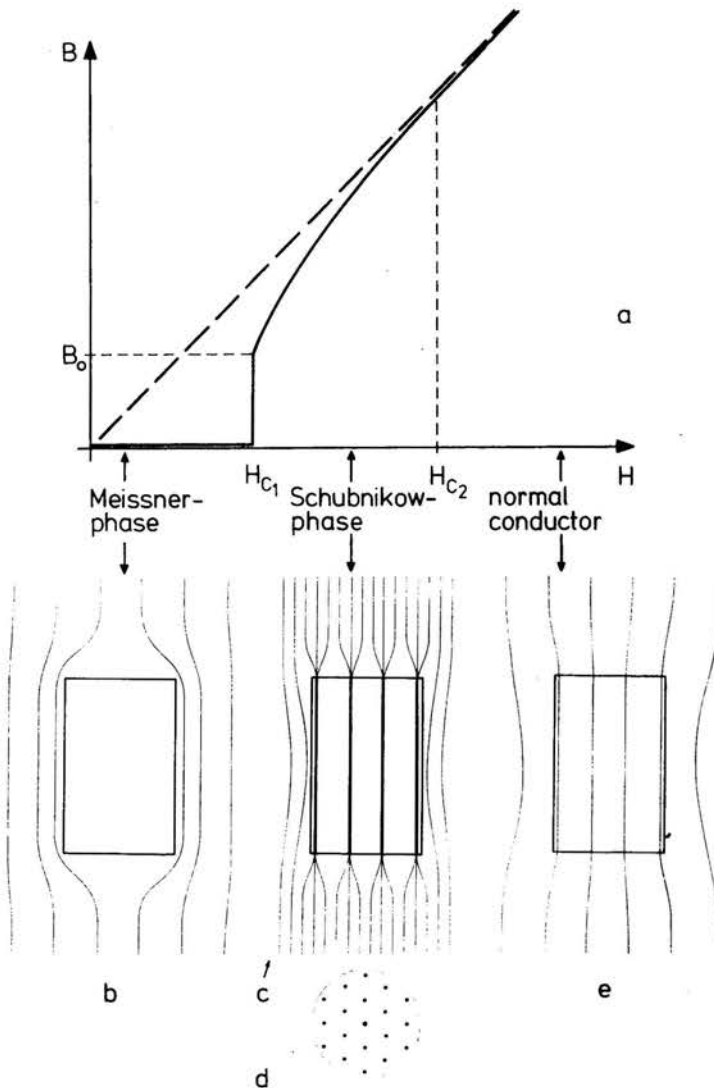


FIG. 5. a) (—) Magnetization curve of an ideal type II superconducting material. Magnetic flux density  $B$  versus the exciting magnetic field  $H$ . (---) Magnetization curve of a normally conducting material. b) Perfect diamagnetism of the Meissner-state. c) Ordered flux line bundle in the Schubnikow-phase. d) Flux line lattice occurring in cross-sections. e) Homogeneous flux distribution in the normal state.

disappears. We arrive at the normal conducting state with homogeneously distributed magnetic flux (Fig. 5e). The region between the two critical fields is called the Schubnikow-phase<sup>(7)</sup>. As the Meissner-phase it is a superconducting phase. But the Schubnikow-phase is characterized by the existence of a magnetic flux line lattice and the stability of the super-

(7) Sometimes the Schubnikow-phase is followed by another superconducting phase which is due to a surface superconductivity. This fact is not important for our problem.

conductivity is closely related to the stability of the flux line lattice<sup>(8)</sup>. Keeping in mind the great technical importance of the superconductivity, I feel that the investigation of the flux line lattice using the field theory is sufficiently motivated.

The phenomena reported hitherto belong to ideal superconductors. In reality we find an irreversible magnetization curve with hysteresis (Fig. 6). This behaviour is due to mechanical eigenstresses in the atomic lattice of the superconducting material. The deviation from the ideal reversible curve depends on the density of eigenstress centres, i.e. mainly on the dislocation density of the atomic lattice.

The irreversible magnetization curve is accompanied by large deformations of the flux line lattice. Just these deformations are of greatest technical importance with respect

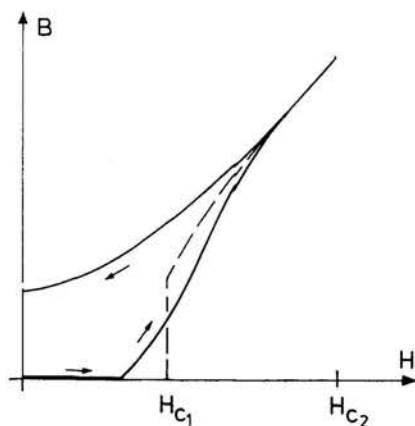


FIG. 6. Irreversible magnetization curve of a real superconductor.

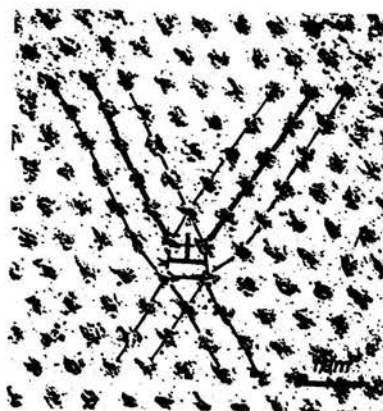


FIG. 7. Edge dislocation in the flux line lattice, leaving the specimen at the top surface. (Micrograph due to TRÄUBLE and ESSMANN [1]).

to the "magnetic hardness" of the material. The classical field theory seems to be an appropriate tool to study these phenomena.

Figure 7 shows an edge-dislocation in the flux line lattice giving rise to characteristic eigenstrains of this lattice. This dislocation extends from the top surface of the specimen into the interior of the flux line bundle (Fig. 12). Figure 8 shows another defect of the flux line lattice, a wedge-disclination which is characterized by a five-fold symmetry within the flux line lattice with a six-fold symmetry. This defect causes a very large eigenstrain and bending of the lattice. The screening of the disclination by means of a cloud of dislocations is another remarkable effect which immediately visualizes the interaction between the disclination and the dislocations. This interaction is due to the overlapping of the respective eigenstrain fields associated with the defects.

In addition to these eigenstrains associated with the eigendefects of the flux line bundle we take into account further the flux bundle strains which are due to defects in the atomic lattice of the material. By means of the interaction between the atomic lattice and the flux line bundle, the flux lines are more or less pinned at atomic lattice defects, giving rise to

<sup>(8)</sup> See below the considerations of flux pinning.

a structure as in Fig. 9. The flux lines get curved and they are hindered during their migration through the specimen; this results in the straining of the flux line lattice. As a consequence it may happen that a flux front appears with a very strongly strained flux line lattice near the front (Fig. 10). Increasing the exciting magnetic field this front penetrates into the probe step by step.

We frequently observe the structure of Fig. 11. On a short distance there occurs a large dilatation gradient of the flux line lattice, i.e. a flux density gradient. From left to right

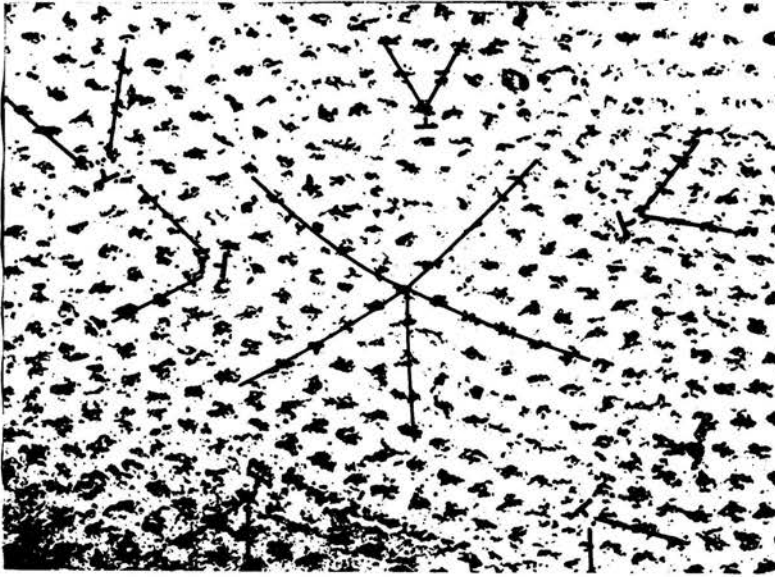


FIG. 8. Screening of a wedge disclination in the flux line lattice by means of flux line lattice dislocations. Illustration of the interaction of different defects. (ANTHONY [12]. Micrograph produced by H. TRÄUBLE and U. ESSMANN).

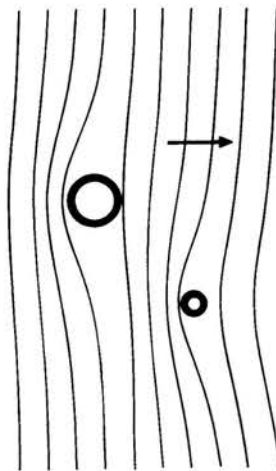


FIG. 9. Pinning of the flux lines at eigenstrain centres of the atomic lattice, for instance at atomic lattice dislocations.

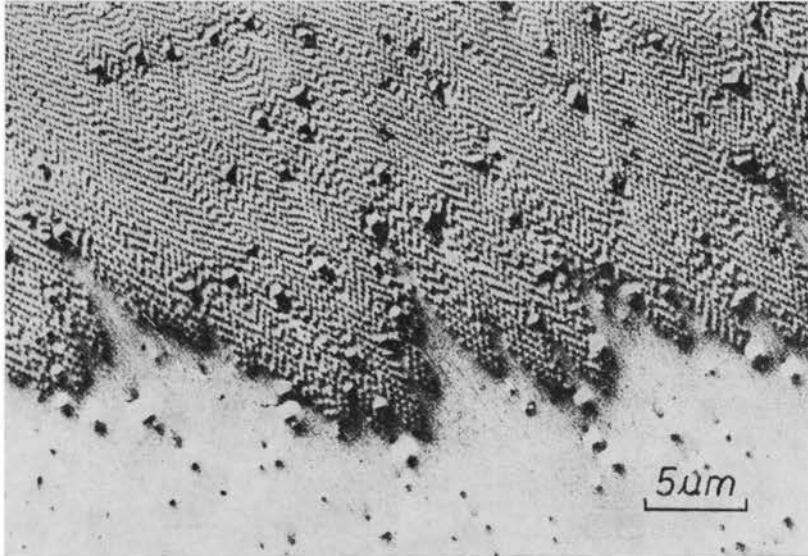


FIG. 10. A flux front penetrating into the specimen illustrates the pinning of the flux bundle at eigenstrain centres of the atomic lattice. (Micrograph due to ESSMANN [26]).

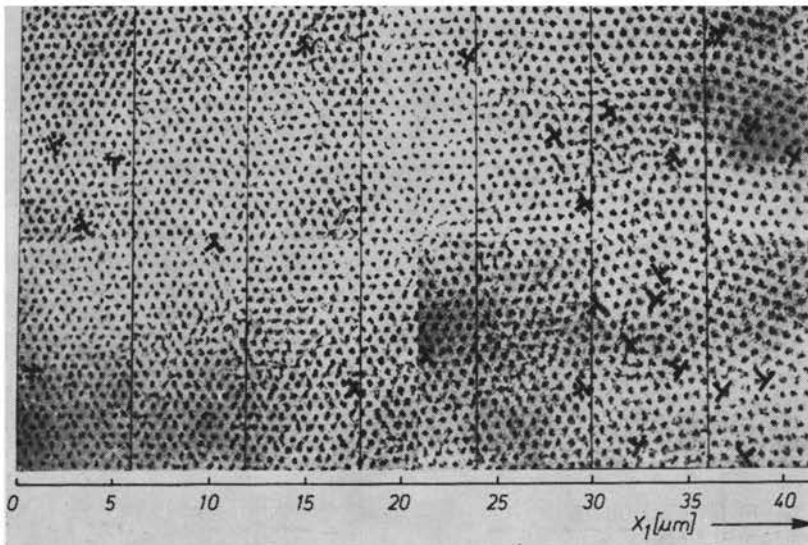


FIG. 11. A flux density gradient of the flux line lattice illustrates the pinning of the flux bundle at eigenstrain centres of the atomic lattice. By means of a large dislocation density in the flux line lattice the strains in the bundle due to flux pinning are mainly cancelled. (Micrograph due to ESSMANN and TRÄUBLE [27]).

we find an increase of the lattice constant of about 100 percent. This effect is directly correlated with the pinning centres of the atomic lattice. Furthermore, we find a large density of flux line lattice dislocations which, with respect to the lattice cell, is about a hundred times larger than common dislocation densities of metals. These dislocations

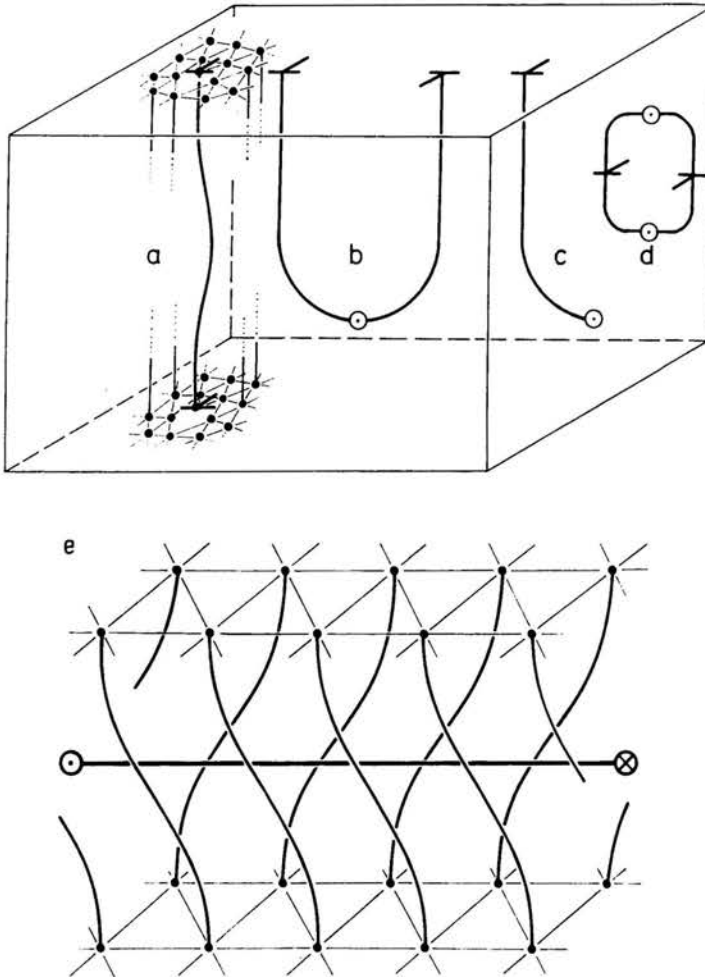


FIG. 12. Curved dislocations in the flux line bundle, the character of which varies between pure edge ( $\perp$ ) and pure screw ( $\odot$ ) Fig. (e) shows schematically the flux line arrangement around a screw dislocation [30].

reduce flux line lattice strains which are due to the pinning of the flux lines in the atomic lattice. Further they seem to be very important for the flux line lattice in order to overcome the flux pinning and to migrate into the specimen: by means of dislocation migration along their gliding planes the flux line bundle is deformed plastically<sup>(9)</sup>. This process is accompanied with flux migration in the specimen [28, 29].

<sup>(9)</sup> This process is analogous to the well-known plastic deformation of atomic crystals.

A final remark concerning the dislocations of Fig. 11: because of the flux pinning we cannot expect that these dislocations run as straight lines from one top surface of the specimen to the other one. We must assume a picture as in Fig. 12: there will be curved dislocations running from one surface to the other (12a), several will return (12b) and several will leave the specimen sideways (12c). Finally, we must expect closed dislocation lines in the interior of flux line bundle (12d).

All defects of the flux line bundle interact with each other and with pinning centres, i.e. with defects of the atomic lattice [23, 28]. The irreversible magnetization curve of the superconductor is the final result of all these interactions. Those interactions related to pinning are the most important ones.

### 3. Some fundamentals concerning the continuum model of the flux line lattice of superconductors

The continuum model of the flux line lattice of superconductors has to fit the discrete structure shown in Fig. 13. A point lattice, representing the atomic lattice, and an ordered line bundle, representing the magnetic flux line lattice penetrate each other. Both subsystems are individually deformable. Nevertheless, they interact with each other.

We compare the “real configuration” (Fig. 13b) of the system with an “ideal configuration” (Fig. 13a), where we have straight and parallel flux lines and where the three-dimensional atomic lattice as well as the two-dimensional flux line lattice are ideal ones. Each deviation from the ideal configuration is assumed to give rise to an “elastic” response of the whole system. I emphasize that in this consideration elastic stresses are located in the flux line lattice as well as in the atomic lattice.

Because of the very large deformations occurring in the flux line lattice, the field theory of the system has to be nonlinear from the very beginning. Nonlinearities must be taken into account with respect to constitutive equations as well as with respect to the deformation theory.

The deformation theory of the point lattice is well established. As far as the deformation theory of the flux line lattice is concerned, I introduced some ideas [25] which are closely related to the fact that the flux line bundle, which so far is the most prominent example of an ordered line bundle, really consists of physical lines which, along the line, exhibit no physical structure at all. As a consequence it is impossible to define each deformation mode commonly used in the deformation theory of point lattices: in Fig. 14 let us first assume that the lines of the bundle possess a physical structure marked by dots. Because of a physical one to one correspondence between the ideal and each deformed configuration (the physical markings are substantially dragged along with the deformation), we are able to distinguish for instance the four deformation modes  $I \rightarrow I, II, III, IV$ . In the next step let us disregard the point structure along the lines. We obtain Fig. 14b; where we can by no means distinguish between the configurations I, II and the ideal state. Configurations III and IV coincide and belong to a two-dimensional compression measured in the cross-sections of the bundle.

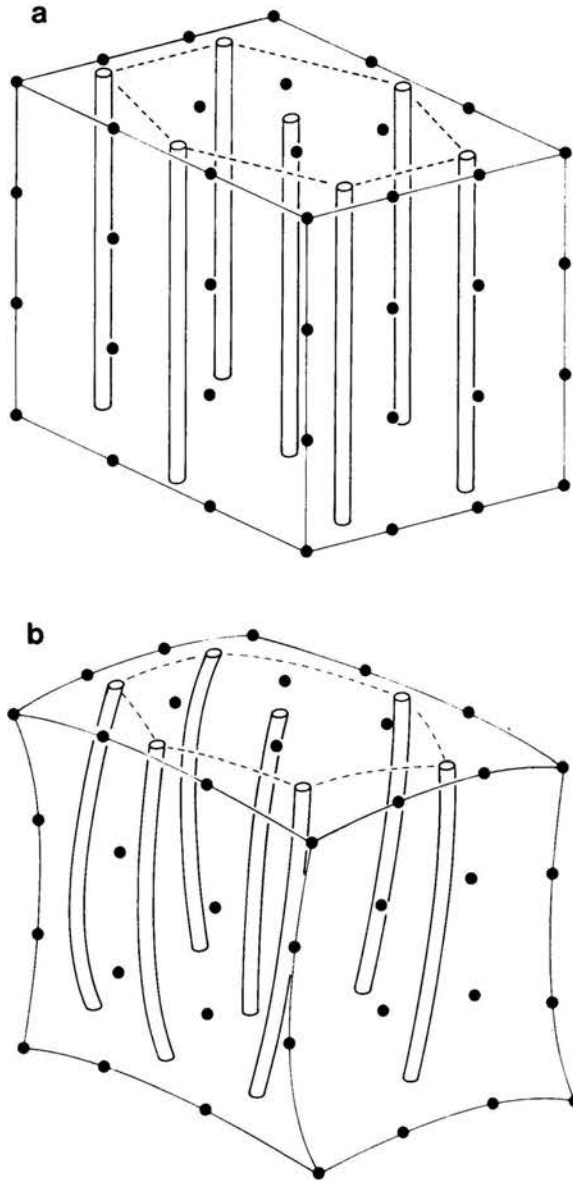


FIG. 13. Schematic structure of the system "flux line lattice + atomic lattice". a) Ideal configuration, b) real (deformed) configuration.

As a consequence neither shear-stresses acting parallel to the bundle nor tensions acting in bundle direction do exist in the ordered line bundle. Such stresses would by definition be related with strains of type I and II in Fig. 14a. But these strains cannot be defined physically. In the ordered line bundle it only makes sense to define curvature and strains occurring in cross-sections of the bundle. Only these deformation modes produce elastic response in the bundle.

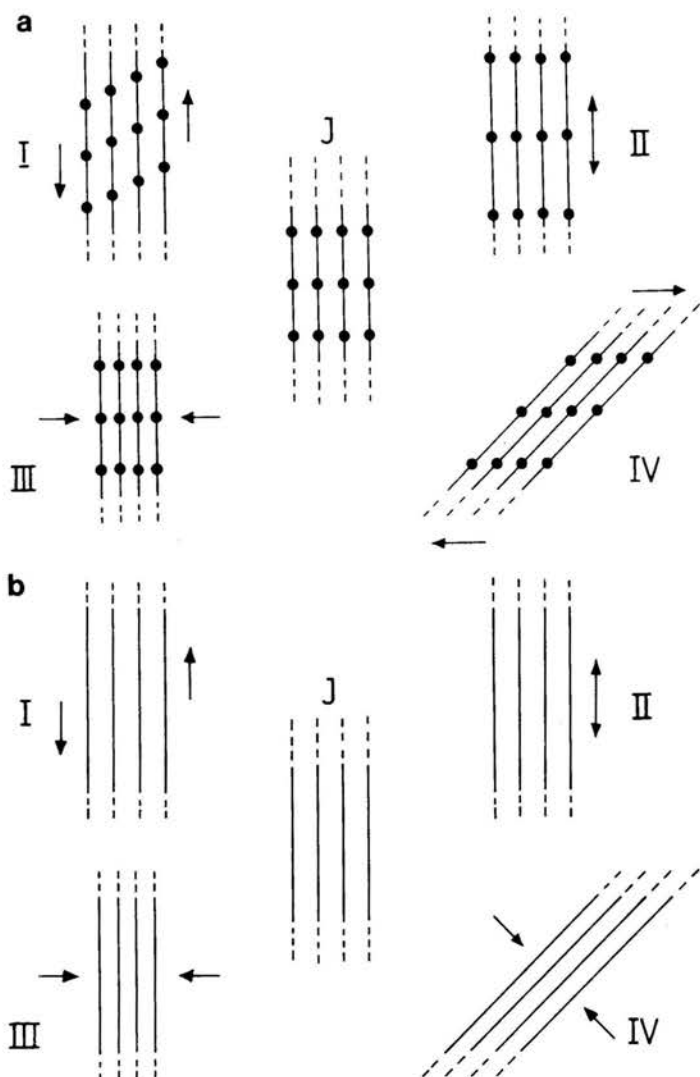


FIG. 14. Not all of the deformation modes of a point lattice can be taken over to the ordered line bundle. In contrast to a) the configurations I and II in b) cannot be distinguished from the ideal configuration I. III and IV get identical configurations which are due to bundle compression measured in cross-sections of the bundle.

#### 4. The bundle model of molten high polymers

Bearing in mind the preceding section, we recognize the bundle model of molten high polymers as another physical realization of the ordered line bundle.

For simplicity let us consider the polyethylen  $C_nH_{2n}$ . The C-atoms arrange themselves in a flat zigzag-structure forming the backbone of the molecule. Each carbon binds two H-atoms (Fig. 15a). These molecules crystallize according to Fig. 15b: parallel molecules

arrange themselves in such a way that the C-atoms form an orthorhombic point lattice with a basis. Alternatively, we may interpret this structure as a molecular bundle with order in the bundle direction. Heating this crystal we finally arrive at the melt, for which Pechhold and Blasenbrey assume that the bundle structure is preserved and only the order

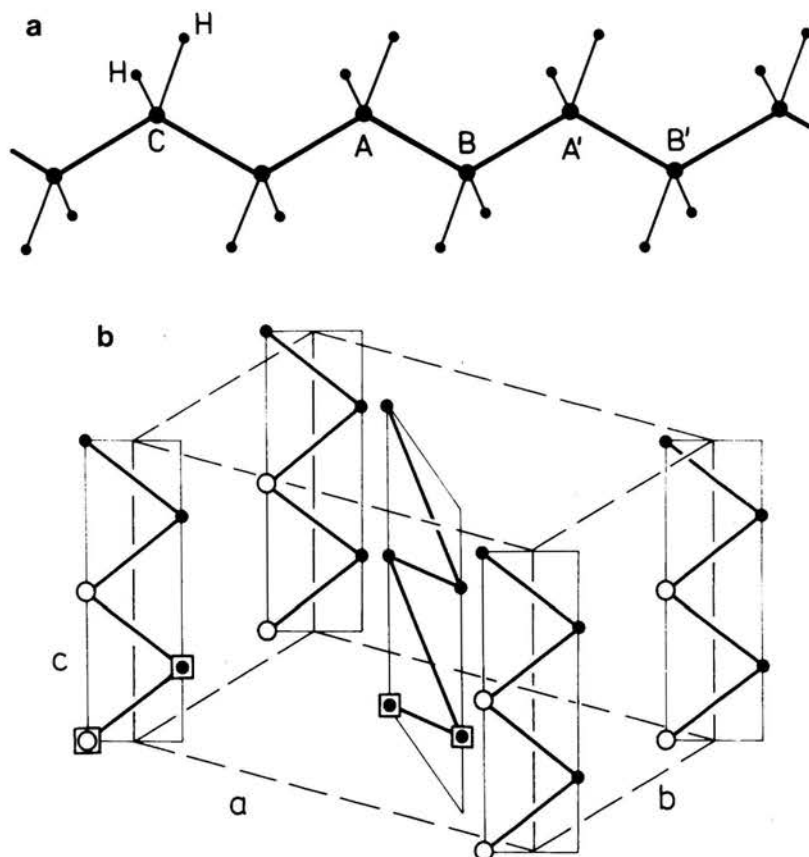


FIG. 15. a) Polyethylen  $C_2H_{2n}$ . b) Crystallized polyethylen. Orthorhombic lattice (○) with basis (□).

along the bundle is destroyed by means of a large density of kinks [19]. They propose the structure shown in Fig. 16.

A kink is a defect in the molecular chain. Because of the second minimum of the rotation potential (Fig. 17a), a single molecule may be transformed from the stable configuration of Fig. 15a into another stable configuration by rotating around the C-C-axis  $AB$  according to an angle of about  $112^\circ$  (Fig. 17b). This configuration has a slightly higher energy compared with the straight molecule. Repeating this procedure in the opposite sense at the C-C-axis  $A'B'$ , we get the kink (Fig. 17c) which is a stable defect with very small<sup>(10)</sup> formation energy of about 0.05 eV and which is associated with the smallest lateral displacement of the molecule [19, 31]. Due to the low formation energy the crystal is endowed

<sup>(10)</sup> "Small" compared with the formation energy of about 1 eV of vacancies in metals (Cu, Al).

in thermal equilibrium with a considerable kink density which increases dramatically at the melting point giving rise to the melting process. This large kink density is visualized in Fig. 16 by means of the irregular zigzag structure.

Since the kinks are roughly fluctuating objects, we cannot define any static order along the molecular bundle. If we mark at a particular instant a volume element as in Fig. 18a, which in principle could be done, we cannot define a static shearing parallel to the bundle (Fig. 18b). The marked element would very rapidly dissolve by means of kink fluctuation which is accompanied with the molecule's migration along the bundle (Figs. 18c, d), i.e. we have no physical tool to measure static shear parallel to the bundle. In consequence there exists no static shear stress acting parallel to the bundle. This fact

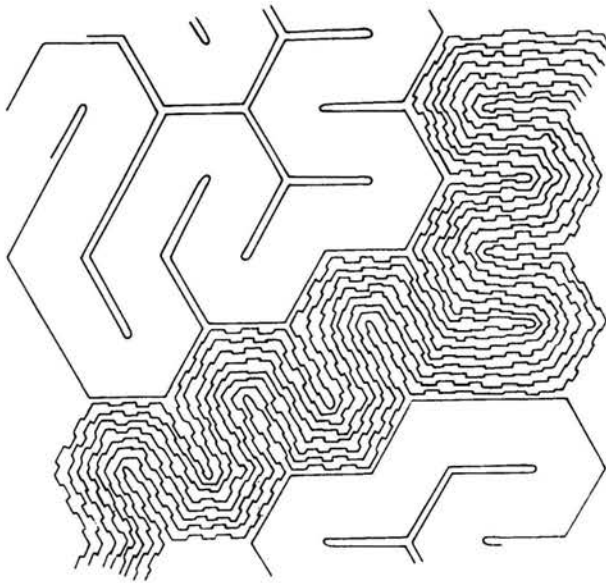


FIG. 16. Bundle and meander model of molten high polymers. Figure due to BLASENBREY and PECHHOLD [19].

corresponds to the fluidity of the polymer melt. Remembering the previous results the molten polymeric bundle thus behaves like an ordered line bundle and the field theory of this model is expected to be a good tool for describing the deformation behaviour of the polymeric melt. This is no trivial program because the mechanical properties of polymeric melts are remarkably different from those of atomic or low molecular melts<sup>(1)</sup>.

The bundle model is extremely anisotropic. In order to find agreement with the observed isotropy on the macroscale, Pechhold and Blasenbrey assumed a meanderlike folding of the molecular bundle (Fig. 16). This meander structure has to be completed randomly into the third dimension. Replacing it by the model system, i.e. by an ordered line bundle, we get the structure of Fig. 19 which includes topological defects at the sites + and - in an otherwise perfect bundle [21, 22]. These defects being disclinations of opposite signs

<sup>(1)</sup> Look for the experiments concerning the shape-memory of the melt [32] or concerning layer structures of the melt [33].

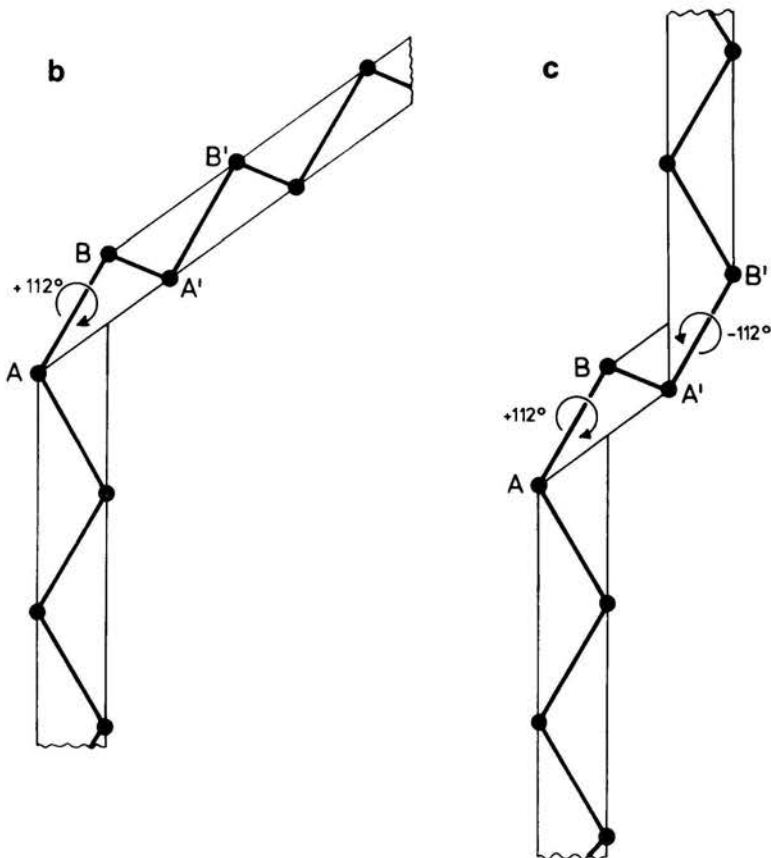
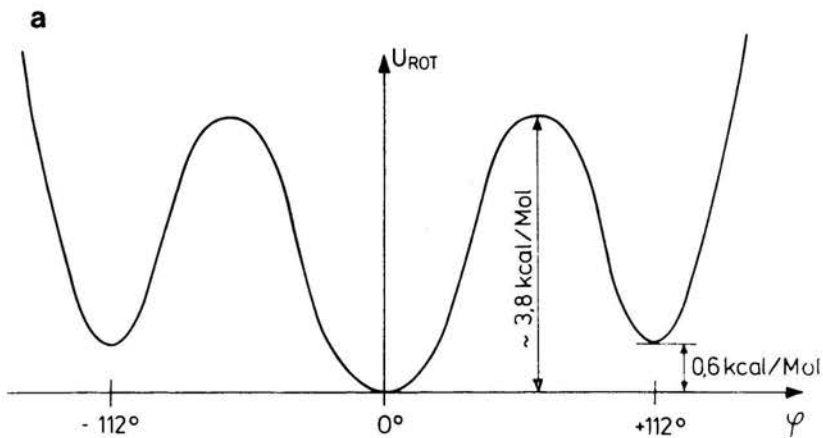


FIG. 17. The kink in a polyethylen molecule is due to the second minimum at  $112^\circ$  of the rotation potential. a) The rotation potential is associated with rotating the molecule around a  $C-C$ -axis ( $AB$  in Fig. 15a). The kink c) is produced by two adjacent "gauche conformations" b) of opposite sense.

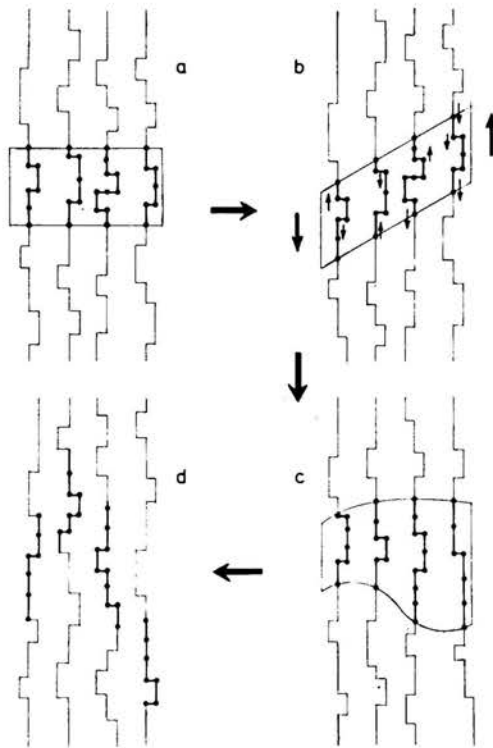


FIG. 18. Because of strong kink fluctuations it is impossible to define a static shear in bundle direction.

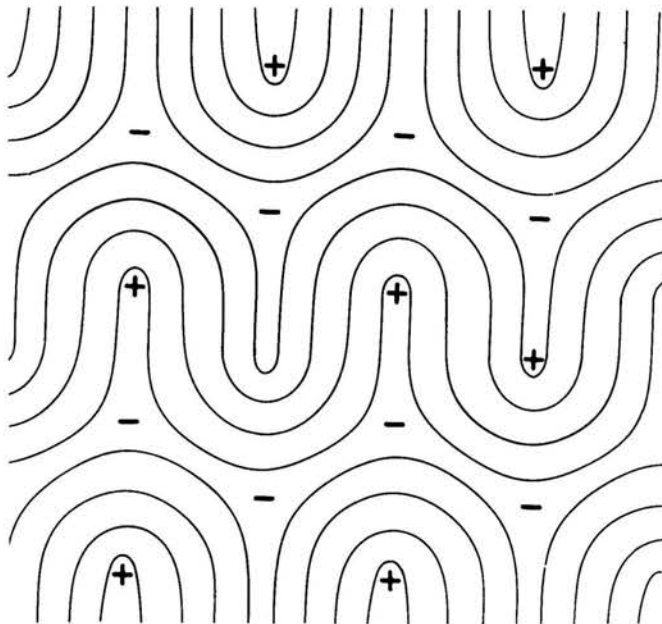


FIG. 19. In terms of the ordered line bundle the meander model is regarded as a multipole disclination arrangement.

are characterized in Fig. 20: a field of directors is associated with the bundle. On a circuit round the disclinations the director suffers a rotation of  $+180^\circ$  and  $-180^\circ$ , respectively<sup>(12)</sup>, giving rise to a closure failure  $\Delta n = n_f - n_s$ . These topological features have to be fitted by means of an appropriate geometrical structure associated with the continuum model

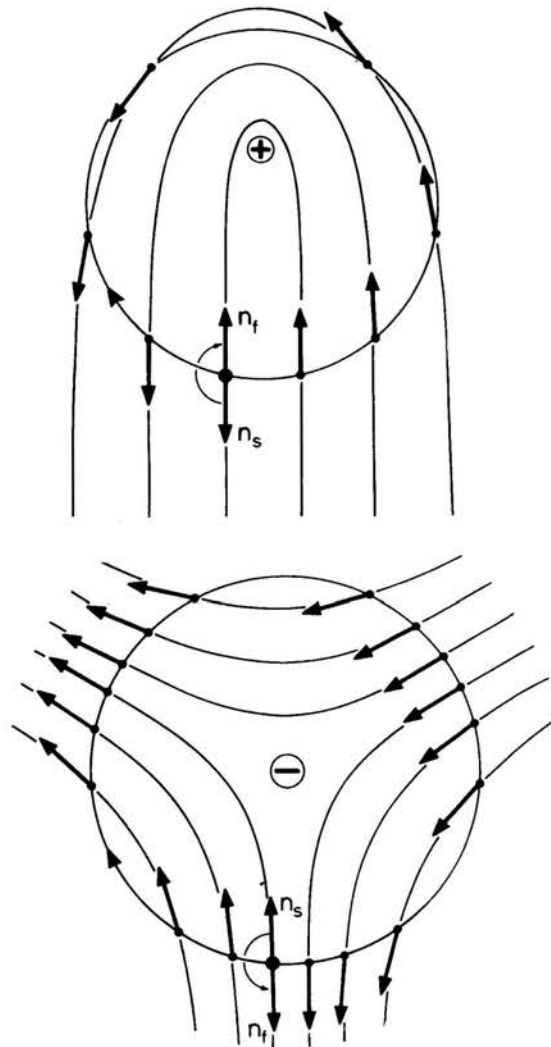


FIG. 20. Two wedge disclinations of opposite signs in the ordered line bundle. On a circuit they are associated with a closure failure of the director.

of the ordered line bundle [25]. Thus the meander model (Fig. 19) may be regarded as a multipole arrangement of disclinations of opposite sign. It is natural to ask for the interactions between these defects and for their effect on the deformation behaviour of the polymer melt.

<sup>(12)</sup> Sense of director rotation as compared with the sense of the circuit.

Figure 21a visualizes that the macroscopic deformation of the melt is associated with a deformation of the disclination grid. Thus, using the meander model we have to expect an elastic response originated by the interaction forces between disclinations. This

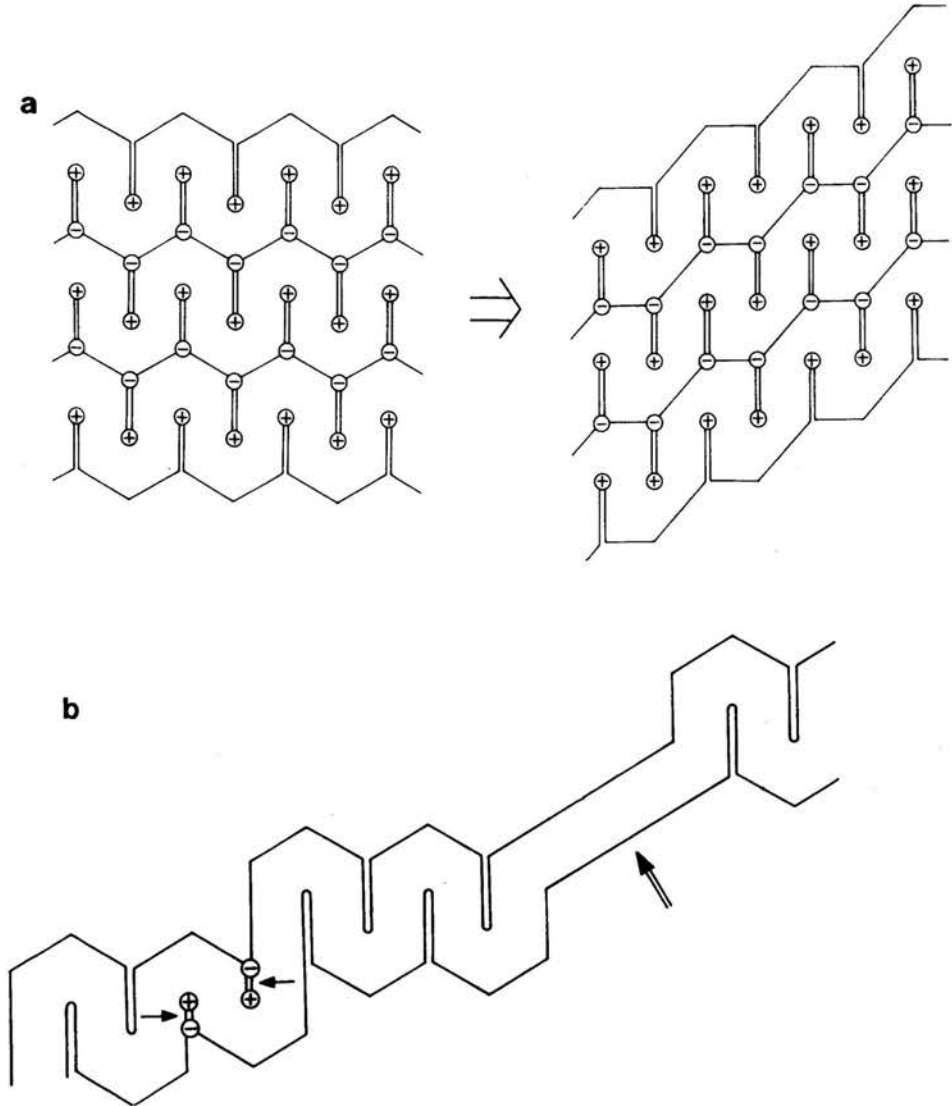


FIG. 21. a) The deformation of the melt is associated with the deformation of the disclination grid, giving rise to an elastic response. b) Annihilation of disclinations associated with bundle stretching.

may be responsible for quite unusual properties of polymeric melts concerning shape stability [32, 33]. An increase of the deformation finally leads to stretching of the molecule bundles. This process is associated with the annihilation of disclinations of opposite sign (Fig. 21b), giving rise to entropy effects, too.

### 5. Problems concerning the field theory of the ordered line bundle

I have established a complete field theory of the ordered line bundle for the static case [25]. Being a nonlinear theory it allows for arbitrary deformations of the system. The constitutive equations are formulated as local equations. They take into account the elastic response associated with line bending and with strain occurring in cross-sections

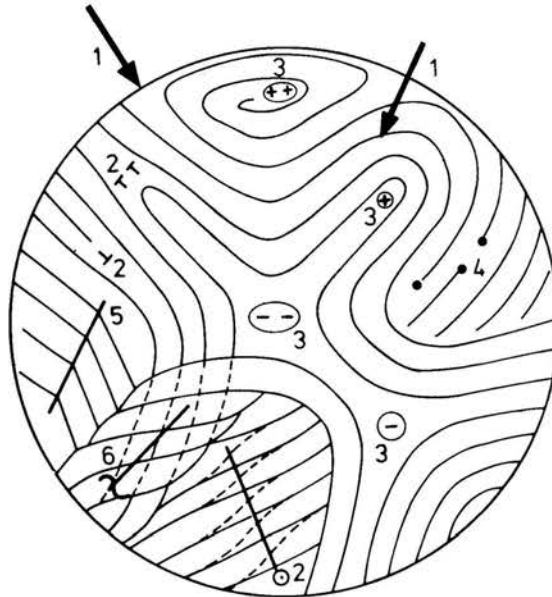


FIG. 22. Some problems which may be studied by means of the field theory of the ordered line bundle. 1) External body and surface forces, 2) dislocations, 3) disclinations, 4) line ends, 5) gauche plains, 6) twisted bundle.

of the bundle. Thermal effects are excluded. The following problems may be solved by means of this theory (Fig. 22):

- a) bundle response with respect to external body and surface forces (1);
- b) eigenstrains produced by bundle defects such as dislocations of different types (2), disclinations of different types (3);
- c) line ends (4);
- d) gauche plains, associated with discontinuous bending (5);
- e) twisted bundles (6)<sup>(13)</sup>.

The theory allows for interactions of all these objects. In the flux line bundle of superconductors the dislocations are of major interest but in the case of polymers we have to deal mainly with disclinations.

Furthermore I established a complete field theory of the magnetic flux line bundle as embedded into the atomic lattice of the superconductor. This theory takes into account the coupling effects due to the strain of the atomic lattice and due to the orientation of the flux bundle with respect to the atomic lattice. It especially allows for the flux pinning.

<sup>(13)</sup> The twisted bundle is closely related to the concept of the "Moebius-crystal".

Up till now our investigations suffer from the fact that we do not know the numerical values of the moduli occurring in the constitutive equations. These values must be determined either by experiment or by more fundamental theoretical investigations. Dynamical experiments may be an appropriate procedure. On the other hand, we may fit the moduli to quantum mechanical calculations in the case of superconductors or to atomic potential calculations in the case of high polymers. So far we have to restrict ourselves to general investigations keeping the moduli unspecified.

As an example Fig. 23 shows an interaction force as calculated by means of the field theory<sup>(14)</sup>: an edge dislocation of the flux line lattice migrating on its glide plane suffers

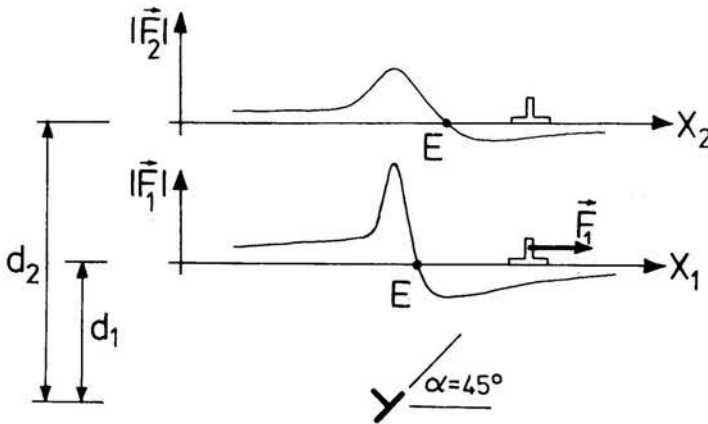


FIG. 23. Interaction force  $F$  between an edge dislocation of the flux line bundle ( $\perp$ ) and an edge dislocation of the atomic lattice ( $\perp$ ). Flux lines and both dislocations are assumed to be straight and parallel.  $X$  is the coordinate of the flux bundle dislocation in its glide plane.  $F$  is a vector in the glide plane acting on the migrating flux bundle dislocation. Calculations are done for a hexagonal triangle flux line lattice and for simplicity we assumed transversal isotropy in the atomic lattice with the axis parallel to the flux lines.

an interaction force  $F(x)$  due to an edge dislocation of the atomic lattice. The flux bundle and both dislocations are assumed to be parallel. The shape of the curve depends on both the distance  $d$  between the glide plane and the atomic lattice dislocation, and on the relative orientation  $\alpha$  of both Burgers vectors<sup>(15)</sup>. The particular points  $E$  mark stable equilibrium configurations of the pair.

Using these results we calculated pinning forces responsible for the irreversible magnetization curve. For instance, a flux bundle dislocation running towards a grain boundary of the atomic lattice suffers a force as shown in Fig. 24 with stable positions at points  $E$ . The most stable position  $E_0$  may be associated with flux pinning and the height  $F_p$  of the adjacent oscillation is interpreted as the pinning force acting on the flux bundle dislocation.

We may further ask for the flux bundle deformations which, as a consequence of the interaction of both subsystems, are due to the strains of the atomic lattice. This question especially arises in the vicinity of an atomic eigenstrain centre (Fig. 9). Such a bundle

<sup>(14)</sup> Figures 23, 24 and 25 are kindly made available by J. BRAUNER [34].

<sup>(15)</sup> Furthermore it depends on the values of the unspecified moduli.



$\mu$  (= moment stress) associated with line bending. Going along a bundle line  $ABC$  and plotting  $\sigma$  and  $\mu$  versus the arc of the line, we find a Gaussian curve for both quantities having its maximum at  $B$ . Increasing the distance from the disclination centre, the curve broadens and the peak is lowered, whereas in the disclination centre the stresses concentrate and get infinitely large.

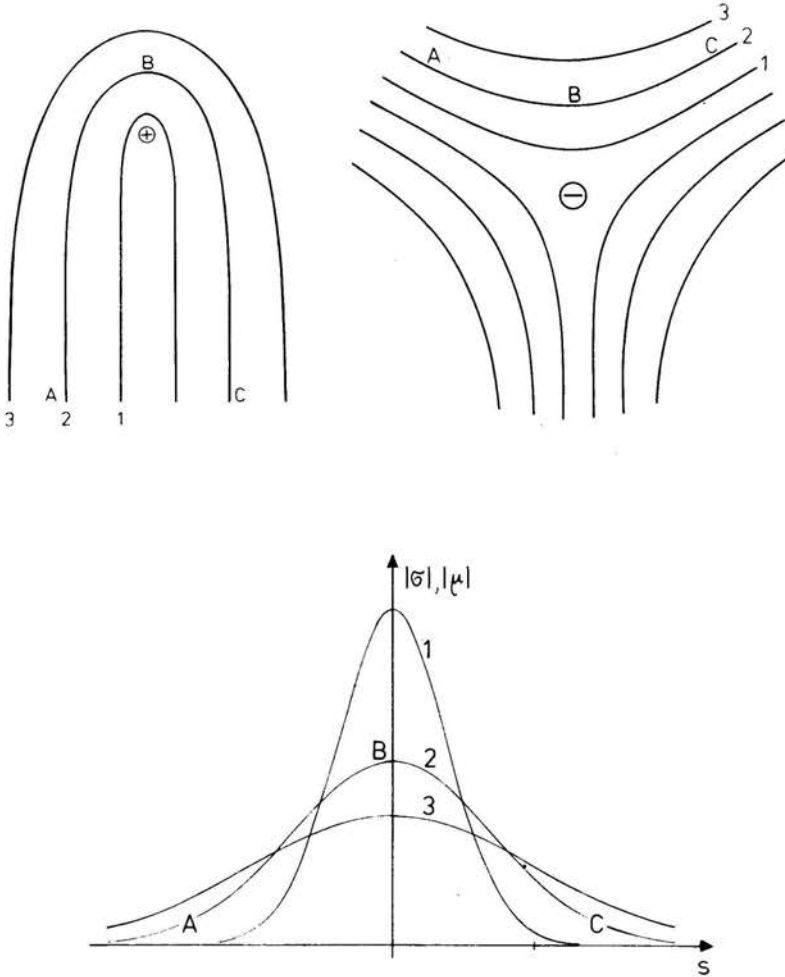


FIG. 26. Stresses in a flat bundle due to  $\pm 180^\circ$  — disclinations. The coordinate  $S$  is the arc along the lines. The stresses of both defects differ only in sign.

## 6. Some remarks on the field theory of the ordered line bundle

My final remarks are concerned with some fundamental mathematical ideas which must be brought in the field theory of the ordered line bundle in order to get a good fit between the discrete physical system and its associated continuum model. This continuum model is a three-dimensional, sufficiently<sup>(17)</sup> continuous point manifold which occupies

<sup>(17)</sup> Continuously differentiable up to a certain order.

the volume of the discrete bundle and which is endowed with several sufficiently continuous mathematical structures. A field of triads is the most fundamental structure of the model. Further structure elements are based on the triad field which fits the field of "bundle triads" of the discrete physical system.

Each configuration of the discrete ordered bundle is described by means of a field of bundle triads. A director  $b$  associated with the bundle direction and two vectors  $b_1, b_2, b_3$  joining neighbouring lines of the ordered bundle build up the triad (Fig. 27a). From the external point of view it is convenient to choose right angles  $\angle(b_1, b_2), \angle(b_1, b_3)$  and a unit vector  $b_1$ . But, as far as physics go, there is really no need for this particular choice. In

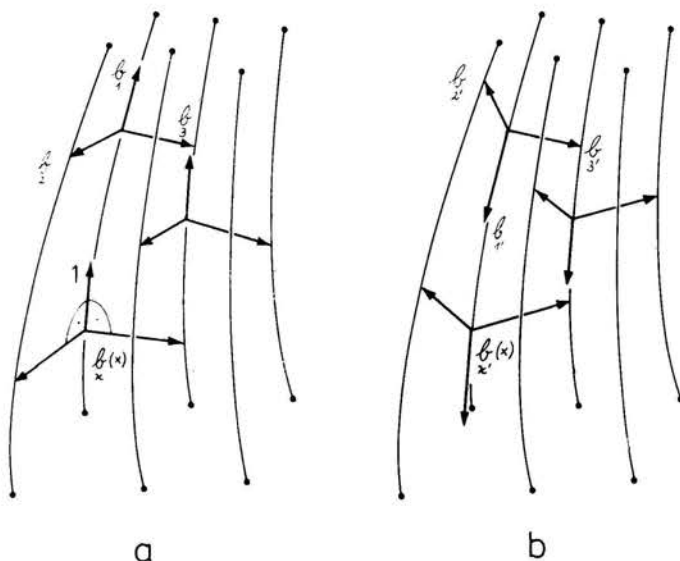


FIG. 27. Fields of bundle triads defining an equivalence class. The totality of all classes is in one-to-one correspondence to all bundle configurations.

contrast to a point lattice where the lattice vectors are uniquely defined by means of the physical structure the lines of the bundle possess no inherent structure. Thus we may equally well introduce each field of triads defining the bundle direction and joining neighbouring lines (Fig. 27b). All these triads are physically equivalent. Each of them includes essential physical information in so far as it defines the bundle configuration. However, it includes furthermore unessential information because of its non-uniqueness. Thus, for a given configuration I define an equivalence class in the usual mathematical sense collecting all physically equivalent fields of triads. All possible bundle configurations are in one-to-one correspondence to the totality of all equivalence classes.

In order to get appropriate physical quantities describing the bundle configuration we have to look for class functions of the equivalence classes. Let me clarify this point by means of an example.

It is well-known that strain tensors are defined as the difference of two metric tensors. This concept holds for the ordered line bundle, too. In this case one of the two metric tensors is defined as follows: let us take a particular field of bundle triads of a given configuration and let us define a metric tensor  $\mathbf{b}$  such that the triads are orthonormalized with

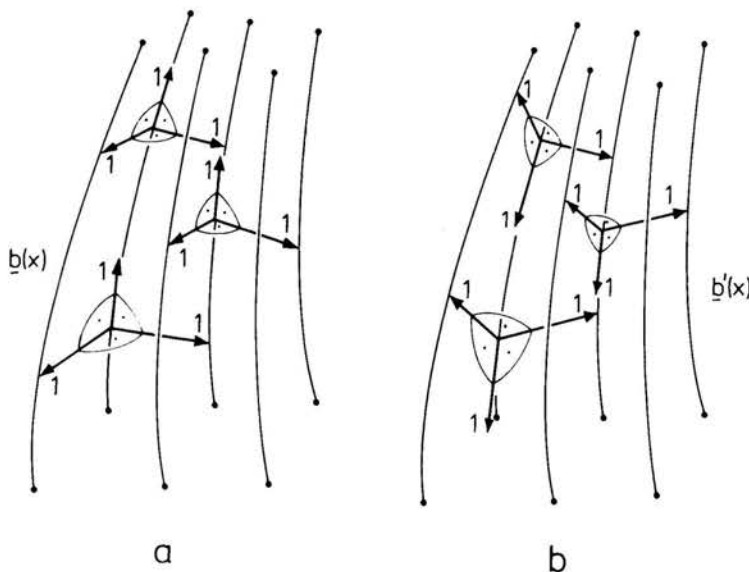


FIG. 28. Definition of regular metric tensors in the bundle.

respect to  $\mathbf{b}$  (Fig. 28a) [11]. In general,  $\mathbf{b}$  is a non-Euclidean metric. Referring to an external coordinate system  $x^i$  its components are uniquely defined by

$$(6.1) \quad b_{ij}(x) = B_i^\alpha(x) B_j^\beta(x) \delta_{\alpha\beta}, \quad (1^8)$$

$B_i^\alpha(x)$  is the inverse of the matrix  $B_\alpha^i(x)$  which defines the components of the vectors  $\mathbf{b}(x)$ ,  $\alpha = 1, 2, 3$ , with respect to the system  $x^i$ . The metric  $\mathbf{b}(x)$  is a regular one, i.e.

$$(6.2) \quad \det \mathbf{b}(x) \neq 0.$$

Performing the same procedure by means of another field of triads  $\mathbf{b}'(x)$  of the same equivalence class, i.e. of the same bundle configuration, we get another regular metric tensor  $\mathbf{b}'(x)$ , by means of which the triads  $\mathbf{b}'(x)$  are orthonormalized (Fig. 28b). In general, the two metrics are different; this means that the regular metric tensors induced by the bundle triads do not define a class function. Nevertheless, all these metric tensors contain a common kernel  $\mathring{\mathbf{b}}(x)$  which I call the "bundle metric" of the ordered line bundle.  $\mathring{\mathbf{b}}(x)$  belongs to each field of triads of the equivalence class, i.e. it is a class function. It is a degenerated non-regular metric

$$(6.3) \quad \det \mathring{\mathbf{b}}(x) = 0,$$

(1<sup>8</sup>) Summation convention implied.

defined by

$$(6.4) \quad \mathring{b}_{ij}(x) = b_{mn}(x)(\delta_i^m - B_{n-1}^m(x))B_i^{\lambda=1}(x)(\delta_j^n - B_{n-1}^n(x)B_j^{\lambda=1}(x)),$$

$$(6.5) \quad \mathring{b}_{ij}(x) = B_i^{\alpha}(x)B_j^{\beta}(x)\mathring{\delta}_{\alpha\beta},$$

$$(6.6) \quad \mathring{\delta}_{\alpha\beta} = \begin{pmatrix} 0 & 0 & 0 \\ 0 & 1 & 0 \\ 0 & 0 & 1 \end{pmatrix}.$$

Equations (6.4) and (6.5) may be evaluated by means of an arbitrary triad  $\mathring{b}(x)$  of the equivalence class and by its associated metric  $\mathring{b}$  (see Eq. (6.1)).  $\mathring{b}(x)$  defines quite unusual metric properties within the ordered line bundle (Fig. 29): all of the directors have the same zero length. The vectors  $\mathring{b}_2$  and  $\mathring{b}_3$  connecting the next neighbour lines are unit vectors.

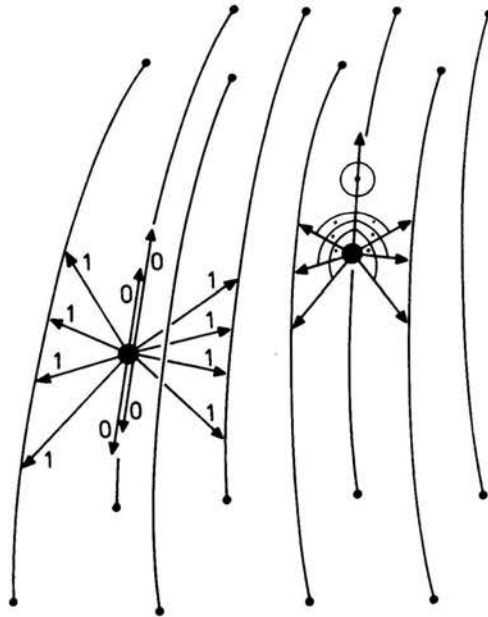


FIG. 29. Strange metric properties of the non-regular bundle metric  $\mathring{b}$ , which is a class function.

At point  $x$  each vector  $\mathring{b}_2(x)$  is perpendicular to each vector  $\mathring{b}_3(x)$  with respect to  $\mathring{b}(x)$ . Finally, the director  $\mathring{b}_1(x)$  is perpendicular to all of the vectors  $\mathring{b}_2(x)$  and  $\mathring{b}_3(x)$ .

Although these metric properties are strange from the point of view of our daily life, they nevertheless are the best fit of a metric structure in the case of an ordered line bundle. Let us imagine a bundle-being living in the bundle and having no external view of the system. Because there is no physical structure on the lines the bundle-being has to orientate itself by means of the line-forest only. It is not able to distinguish the vectors  $\mathring{b}_2$  and  $\mathring{b}_{2'}$  (Fig. 27) by physical means. Therefore it seems quite natural for the bundle-being to associate the

same length (say length 1) with all these vectors. Missing physical marks on the lines it is again reasonable to associate zero length with all directors.

The bundle metric  $\mathring{\mathbf{b}}(x)$  of a deformed bundle configuration can be associated with the ideal configuration of the bundle, too. In the ideal configuration the Euclidean distance between adjacent lines is the same every-where (say length 1). Deforming the configuration of Fig. 29 into the ideal configuration and dragging along the metric properties with respect to  $\mathring{\mathbf{b}}$  we confirm the following statement:  $\mathring{\mathbf{b}}$  measures Euclidean distances occurring in cross-sections of the bundle after the bundle (at least locally) has been transformed into the ideal configuration. Thus it is obvious that  $\mathring{\mathbf{b}}$  is an appropriate quantity to define strains of the bundle.

Some final remarks are concerned with deformations of the bundle. Being a physical object each line on the whole may be identified in each configuration (Fig. 30). But because

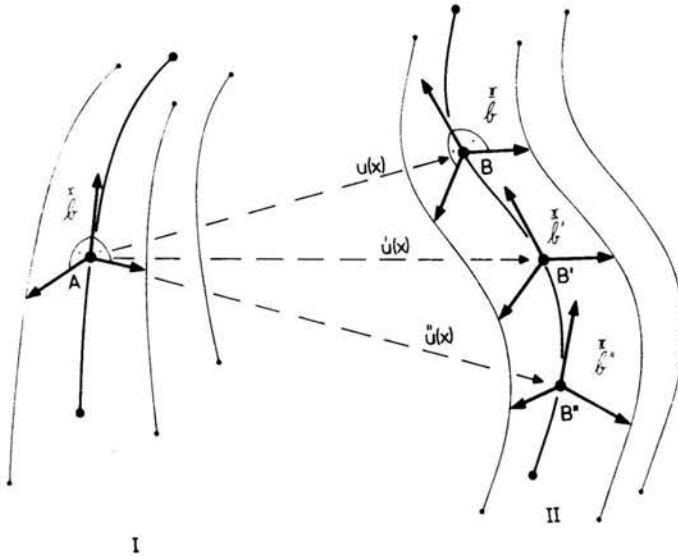


FIG. 30. The deformation of an ordered line bundle is associated with an equivalence class of displacement fields.

there is no inherent physical structure available on the lines we cannot define a unique physically motivated point to point relation between both configurations. As a consequence it is impossible to define a material coordinate system which is dragged along with the deformed bundle. Furthermore, we cannot define a unique displacement field  $\mathbf{u}$  which carries one configuration into the other one. Consequently, we do not know which of the triads  $B$ ,  $B'$ ,  $B''$  should be associated with the triad  $A$  (Fig. 30). To solve these problems I again introduced another set of equivalence classes. Each of these classes is associated with a particular pair of configurations of the same bundle. It includes all displacement fields belonging to the pair of configurations.

Thus the deformation theory of the ordered line bundle is ruled by the equation

$$(6.7) \quad \{\mathring{\mathbf{b}}^{\text{I}}(x)\} \stackrel{\{\mu(x)\}}{\sim} \{\mathring{\mathbf{b}}^{\text{II}}(x)\}.$$

The equivalence class of triads  $\{\overset{I}{b}(x)\}$  belonging the first configuration is transformed into the class  $\{\overset{II}{b}(x)\}$  of the second configuration by means of the equivalence class  $\{u(x)\}$  of displacement fields.

The concept of equivalence classes rules the whole theory, its geometrical as well as its constitutional structure.

My participation at the conference in Jodłowy Dwór, Poland, was sponsored by the Deutsche Forschungsgemeinschaft. I highly appreciate this support.

## References

1. H. TRÄUBLE and U. ESSMANN, *Phys. Stat. Sol.*, **25**, 373, 1968.
2. K. KONDO, *Proc. of the 2<sup>nd</sup> Japan National Congr. Appl. Mech.*, **41**, 1952.
3. B. A. BILBY, R. BULLOUGH and E. SMITH, *Proc. Roy. Soc. London, Ser. A* **236**, 481, 1956.
4. E. KRÖNER, *Kontinuumstheorie der Versetzungen und Eigenspannungen*, *Erg. d. Angew. Math. Bd. 5*, Berlin, Göttingen, Heidelberg; Springer, 1958.
5. E. KRÖNER, *Arch. Rat. Mech. Anal.*, **4**, 273, 1960.
6. E. KRÖNER and A. SEEGER, *Arch. Rat. Mech. Anal.*, **3**, 97, 1959.
7. C. TEODOSIU, *Rev. Roum. Sci. Techn., Série Méch. Appl.*, **12**, 961, 1967.
8. C. TEODOSIU, *Rev. Roum. Sci. Techn., Série Mech. Appl.*, **12**, 1061, 1967.
9. C. TEODOSIU, *Rev. Roum. Sci. Techn., Série Mech. Appl.*, **12**, 1291, 1967.
10. R. STOJANOVITCH, *Phys. Stat. Sol.*, **2**, 566, 1962.
11. K. H. ANTHONY, *Arch. Rat. Mech. Anal.*, **37**, 161, 1970.
12. K. H. ANTHONY, *Arch. Rat. Mech. Anal.*, **39**, 43, 1970.
13. B. A. BILBY, L. R. T. GARDNER, A. GRINDBERG and M. ZÓRAWSKI, *Proc. Roy. Soc.*, **A 292**, 105, 1966.
14. K. H. ANTHONY, *Arch. Rat. Mech. Anal.*, **40**, 50, 1971.
15. A. SEEGER, *Theorie der Gitterfehlstellen*. *Handbuch der Physik (Flügge)*, Bd. VII. 1, Berlin, Göttingen, Heidelberg; Springer, 1955.
16. F. R. N. NABARRO, *Theory of crystal dislocations*, Oxford, At the Clarendon Press, 1967.
17. A. SEEGER, *Kristallplastizität*, *Handbuch der Physik (Flügge)*, Bd. VII. 2, Berlin, Göttingen, Heidelberg; Springer, 1958.
18. W. BUCKEL, *Supraleitung*, Weinheim; Physik Verlag, 1972.
19. S. BLASENBREY and W. PECHHOLD, *Berichte der Bunsengesellsch. für physikalische Chemie*, **74**, 784, 1970.
20. P. G. DE GENNES, *The Physics of Liquid Crystals*, Clarendon Press, Oxford 1974.
21. K. H. ANTHONY and E. KRÖNER, In: *Deformation and Fracture of High Polymers* (Ed. Kausch, Hassell, Jaffee). Battelle Institute Materials Science Colloquia, Kronberg, Germany, 1972. Plenum Press, New York, London 1973.
22. K. H. ANTHONY and E. KRÖNER, *Kolloid-Zeitschr. und Zeitschr. Polymere*, **251**, 813, 1973.
23. K. H. ANTHONY, J. BRAUNER, O. EBERHARDT and E. KRÖNER, *Proc. of the Intern. Discussion Meeting on Flux Pinning in Superconductors*. (Ed. HAASEN, Freyhardt). Akademie der Wissenschaften in Göttingen 1974.
24. J. A. SCHOUTEN, *Ricci-Calculus*, Springer, Berlin-Göttingen-Heidelberg 1954.
25. K. H. ANTHONY, *Feldtheorie physikalischer Linienstrukturen*, Habilitations-thesis, Universität Stuttgart 1974.
26. U. ESSMANN, *Physica*, **55**, 83, 1971.
27. U. ESSMANN and H. TRÄUBLE, *Phys. Stat. Sol.*, **32**, 337, 1967.

28. R. SCHMUCKER, Dr-thesis, Universität, Stuttgart 1974.
29. U. ESSMANN and R. SCHMUCKER, Phys. Stat. Sol. (b), **64**, 603, 1974.
30. R. LABUSCH, Physics Letters, **22**, 9, 1966.
31. P. C. HÄGELE, Dr-thesis, Universität, Ulm 1972.
32. R. HOSEMANN, J. LOBODA-CACKOVCI and H. CACKOVIC, Zeitschr. Naturforsch., **27**, 478, 1972.
33. J. PETERMAN and H. GLEITER, Phil. Mag., **28**, 271, 1973.
34. J. BRAUNER, Dr-thesis in preparation, Universität Stuttgart [to be published].
35. F. FALK. Diplom-thesis, Universität Stuttgart 1973 [to be published].
36. K. H. ANTHONY and A. SEEGER, Phil. Mag., **28**, 1125, 1973.

INSTITUT FÜR THEORETISCHE UND ANGEWANDTE PHYSIK  
UNIVERSITÄT STUTTGART, GFR.

*Received November 11, 1975.*